Fibrillation of Human Insulin A and B Chains

Dong-Pyo Hong, Atta Ahmad, and Anthony L. Fink*

Department of Chemistry and Biochemistry, University of California, Santa Cruz, California 95064

Received March 12, 2006; Revised Manuscript Received June 5, 2006

ABSTRACT: Human insulin, which consists of disulfide cross-linked A and B polypeptide chains, readily forms amyloid fibrils under slightly destabilizing conditions. We examined whether the isolated A and B chain peptides of human insulin would form fibrils at neutral and acidic pH. Although insulin exhibits a pH-dependent lag phase in fibrillation, the A chain formed fibrils without a lag at both pHs. In contrast, the B chain exhibited complex concentration-dependent fibrillation behavior at acidic pH. At higher concentrations, e.g., >0.2 mg/mL, the B chains preferentially and rapidly formed stable protofilaments rather than mature fibrils upon incubation at 37 °C. Surprisingly, these protofilaments did not convert into mature fibrils. At lower B chain concentrations, however, mature fibrils were formed. The explanation for the concentration dependence of B chain fibrillation is as follows. The B chains exist as soluble oligomers at acidic pH, have a β-sheet rich conformation as determined by CD, and bind ANS strongly, and these oligomers rapidly form dead-end protofilaments. However, under conditions in which the B chain monomer is present, such as low B chain concentration (<0.2 mg/mL) or in the presence of low concentrations of GuHCl, which dissociates the soluble oligomers, mature fibrils were formed. Thus, both A and B chain peptides can form amyloid fibrils, and both are likely to be involved in the interactions leading to the fibrillation of intact insulin.

Many proteins can misfold and form intracellular or extracellular aggregates that cause cellular dysfunction, and the misfolding of more than 20 proteins is associated with amyloid fibril diseases (*1*−*3*). In fact, it has been suggested that the ability to form fibrils may be a generic property of the polypeptide backbone, although the propensities of different sequences to form such species can differ widely (*4*−*6*). So far, a number of studies have been reported on key features of amyloid fibrillation: (i) identifying residues critical for aggregation (*7*−*11*), (ii) identifying factors that lead to inhibition or enhancement of fibrillation (*12*−*14*), (iii) characterization of hierarchical assemblies, such as protofilaments, protofibrils, and fibrils, in the fibrillation pathway (*15*−*17*), and (iv) studying molecular-level structure of amyloid fibrils (*18*) by using X-ray diffraction (*19*), solid-state NMR (*20*, *21*), FTIR (*22*), and H−D exchange (*23*, *24*). However, the detailed mechanisms underlying the formation of fibrils still remain unclear.

Insulin is a small helical protein hormone consisting of two polypeptides, the A chain (21 residues) and the B chain (30 residues), linked together by two interchain disulfide bridges (Figure 1A), and undergoes fibrillation at elevated temperatures, at low pH, and in the presence of organic solvents and agitation (*25*−*29*). Fibrillation poses a variety of problems in the production, storage, and delivery (especially via insulin pumps) of soluble insulin. For example, during the preparation of recombinant insulin for clinical use, it is subjected to low pH, agitation, and organic solvent, all conditions that favor fibrillation.

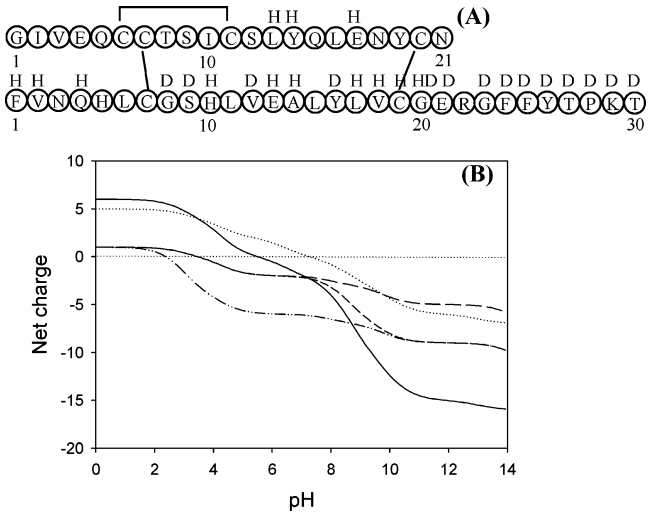

FIGURE 1: (A) Amino acid sequence and location of the disulfide bonds of human insulin. The superscripts indicate the amino acid residues involved in association of insulin into dimers (D) and hexamers (H). (B) Protein net charge as a function of pH: insulin (—), B chain (•••), A chain (- - -), RCAM-Ach (− − −), and RCM-Ach (−••−).

In solution, insulin can exist as monomers, dimers, tetramers, hexamers, and possibly higher associated states, depending on concentration, pH, metal ions, ionic strength, and solvent composition (*30*, *31*). It has been proposed that insulin fibrillation occurs through the dissociation of oligomers into the monomer and the monomer undergoes a structural change, developing a strong propensity for fibrillation (*25*−*30*).

* To whom correspondence should be addressed: Department of Chemistry and Biochemistry, University of California, Santa Cruz, CA 95064. Telephone: (831) 459-2744. Fax: (831) 459-2935. E-mail: fink@chemistry.ucsc.edu.

10.1021/bi0604936 CCC: $33.50
Published on Web 07/11/2006

X-ray analysis of the insulin hexamer reveals that the A chain consists of two helical segments, A2−A8 and A13−A20, the B chain includes a region of extended structure (B1−B8), an α-helical region between residues B9 and B19, a β-turn (B20−B23), and, finally, another extended strand between residues B24 and B28 (*32*). From studies of the effects of mutations in insulin on its kinetics of fibrillation, Nielsen et al. (*33*) identified two surfaces on the insulin monomer as potential interacting sites in insulin fibrils, one consisting of residues B10, B16, and B17 (all on one β-strand) and the other consisting of at least residues A8 and B25, observed from data on the fibrillation of insulin mutants. Since possible effects of the mutations on the stability or dynamics of the monomer were not investigated, these conclusions regarding the interaction sites in the fibril should be regarded as tentative. Cryoelectron microscopy has been used to characterize insulin fibrils: low-resolution three-dimensional structures of fibrils revealed a compact shape for the insulin protofilament (two, four, or six per fibril), with the cross-β structure composed of relatively flat β-sheets (*34*). The solution structure of human insulin under amyloidogenic conditions (pH 2.4 and 60 °C) has been determined using NMR (*35*). In this structure, the N-terminal segments of the A and B chains are separated from the core, and unfolding of the N-terminal helix of the A chain exposes a hydrophobic surface, suggesting a potential initial interaction surface for aggregation. In contrast, the C-terminus of the B chain remains attached to this partial helical core. The solution conformation of des-(B26−B30)-insulin determined by NMR has been compared to that derived from crystallography; whereas the overall structure is retained in solution, a high degree of flexibility at the N-terminal part of the A chain and at the N-terminal and C-terminal parts of the B chain was observed (*36*). Crystallographic studies of human insulin at pH 2.1 in the presence of sulfate demonstrate that the native fold is maintained at low pH. The bound sulfate ions are associated with local deformations in the protein, suggesting that the structure is more flexible at low pH (*37*). Thus, the identification of the specific regions of the insulin molecule involved in aggregation remains to be determined. The potential for fibrillation of the isolated A and B chains also has not been examined.

Several models for fibril formation have been proposed. The most common is the nucleated polymerization, in which a rare event leads to formation of a nucleus (usually considered to be a small oligomer, but in principle it could be a rare monomer conformation) that once formed very rapidly leads to the formation of the beginning of a "fibril". The smallest such entity, often thought to consist of two parallel β-sheets, is called a protofilament. Protofilaments can wrap around each other to form protofibrils or mature fibrils, which are usually considered to be composed of two to six protofilaments. One model assumes that the protofilaments grow simultaneously in place in the mature fibril; i.e., the growing face of the mature fibril has the protofilaments in place. Alternate models include formation of oligomers (protofibrils) that line up and "snap together" to form fibrils.

In this study, to improve our understanding of the mechanism of insulin fibrillation, insulin was reduced and the A and B chains were isolated. The fibrillation behavior of the two chains was examined in terms of the kinetics and fibril/aggregate morphologies. We used thioflavin T, a dye that has the useful property of binding relatively specifically to amyloid fibrils with an associated large enhancement in its fluorescence quantum yield, to monitor the kinetics of fibril formation. We used the fluorescent hydrophobic dye ANS to detect the presence of partially folded intermediates, since this compound is well-known to bind to partially folded conformations with an enhancement of its fluorescence, including a blue shift in its emission maximum. Our results indicate that although the A chain formed amyloid fibrils readily without a lag phase, the B chain formed either stable protofilaments or mature fibrils depending on the experimental conditions, implying that both chains may play important roles in the fibrillation of intact insulin.

MATERIALS AND METHODS

Materials. Monocomponent human insulin (batch HO1713) was obtained from Novo Nordisk A/S. The zinc content was 0.4% (w/w of insulin), corresponding to approximately two Zn^{2+} atoms per insulin hexamer. ANS,[1] iodoacetic acid, and iodoacetamide were purchased from Sigma (St. Louis, MO). Thioflavin T (ThT) was obtained from Fluka.

Purification of Insulin A and B Chains. Human insulin (4 mg) was dissolved in 1 mL of 50 mM potassium phosphate buffer (pH 7.4) containing 1 mM EDTA and 10 mM DTT, as described previously (*38*). This was kept at room temperature for 1 day, at which time the B chain precipitated, and the A chain remains soluble. The reaction mixture was centrifuged at 14 000 rpm for 30 min. The A chain in the supernatant was separated from residual reagents on a Sephadex G-25 column. Because the A chain peptide at high concentrations rapidly formed fibrils, it was prepared at 0.5 mg/mL and used at that concentration in fibrillation experiments immediately after its purification. The pellet containing mainly the B chain was washed with water at least three times to remove the intact insulin and DTT. The presence of intact insulin in the supernatant of the washed pellet was monitored with SDS−PAGE; when the pellet had been washed three times, no intact insulin was observed in the supernatant.

Alkylation of A Chain Thiol Groups. Alkylation of the thiol groups of the reduced A chain was achieved by addition of an excess of iodoacetamide or iodoacetic acid (~0.1 M) over the thiol groups. The reaction was continued for 2 h, and then the alkylated A chain was separated from residual reagents on a Sephadex G-25 column. The alkylation of the thiol groups of the A chain was confirmed by titration with 5,5′-dithiobis(2-nitrobenzoic acid) (DTNB). The B chain and RCM-Ach were insoluble at pH 7.5 and 1.6, respectively; thus, we could not carry out fibrillation experiments under these conditions.

To study the relationship between net charge and solubility, we calculated the net charges of the A and B chains and their alkylated forms assuming independence of titratable groups based on the pK_{int} values as a function of pH (Figure 1B). The pI (isoelectric point) values for the B chain and

[1] Abbreviations: ANS, 1-anilinonaphthalene-8-sulfonic acid; CD, circular dichroism; DTNB, 5,5′-dithiobis(2-nitrobenzoic acid); EM, electron microscopy; RCAM-Ach, reduced and carboxamidomethylated insulin A chain; RCM-Ach, reduced and carboxymethylated insulin A chain; ThT, thioflavin T; GuHCl, guanidine hydrochloride.

RCM-Ach were ~7.2 and ~2.3, respectively, suggesting that the limited solubility in the vicinity of the pI was responsible for their formation of insoluble aggregates at the corresponding pH values.

Kinetics of Fibrillation Monitored by Thioflavin T Fluorescence. All protein samples were freshly prepared immediately prior to the experiments. Insulin was dissolved at a concentration of 2 mg/mL in the appropriate buffer, and its concentration was determined by the absorbance at 276 nm using an extinction coefficient of 1.08 for 1.0 mg/mL. The extinction coefficients (ϵ) for insulin A and B chains were calculated from their amino acid sequences. Fibril formation was studied in solutions of 25 mM HCl, 100 mM NaCl (pH 1.6), or 50 mM phosphate buffer (pH 7.5). A stock solution of ThT was prepared at a concentration of 1 mM in distilled water and stored at 4 °C protected from light. For in situ ThT fluorescence measurements, 10 μM ThT was added to each of the protein solutions to be incubated in the 96-well plate; 100 μL sample volumes were added to each well. Five replicates were measured for each sample to minimize the well-to-well variation. The plate was covered with a Mylar plate sealer and incubated at 37 °C. The plate was subjected to continuous agitation except for readings at 15 or 30 min intervals, with the speed of agitation being 600 rpm and the shaking diameter being 1 mm. The fluorescence measurements were performed on a Fluoroskan Ascent CF fluorescence plate reader (Thermo Labsystems). The fluorescence was measured with excitation at 450 nm and emission at 485 nm and curve-fit as described previously (*28*).

Supernatant Studies. After fibrillation, all samples were centrifuged at 14 000 rpm for 30 min, and proteins in the supernatant and pellet were analyzed with the Lowry assay. In addition, the concentration of ThT in the supernatant was determined using a Shimadzu UV spectrometer (model UV-2401PC) at 412 nm.

Circular Dichroism Measurements. CD spectra were obtained with an AVIV (Lakewood, NJ) 60DS spectrophotometer. Spectra were recorded in a 0.1 cm path length round cell from 250 to 190 nm. For all spectra, an average of five scans was obtained. CD spectra of the appropriate buffers were recorded and subtracted from the protein spectra.

ANS Fluorescence Measurements. The effect of various concentrations of GuHCl on the binding of ANS to insulin and the B chain was studied. Protein (1 mg/mL) was dissolved in 0.025 M HCl and 0.1 M NaCl at pH 1.6 with 10 μM ANS. The samples were incubated at room temperature for 20 min. The ANS fluorescence spectra were measured with a FluoroMax-3 spectrofluorometer from 360 to 600 nm (excitation at 350 nm).

Seeding Experiments for B Chain Fibrillation. Amyloid fibrils of the B chain peptide were used as seed fibrils in the seeding experiments. When fibrillation was complete, as described above, the fibril solution (2 mg/mL) was centrifuged at 14 000 rpm for 30 min. After the supernatant was removed, the pellet was resuspended in water and sonicated. The effect of seeding on the kinetics of fibrillation was studied by adding 10% preformed seed fibrils.

Electron Microscopy. Transmission electron micrographs were collected using a JEOL JEM-100B microscope operating with an accelerating voltage of 80 kV. Typical nominal magnifications ranged from 30000× to 75000×. Samples were deposited on Formvar-coated 300 mesh copper grids and negatively stained with 1% aqueous uranyl acetate.

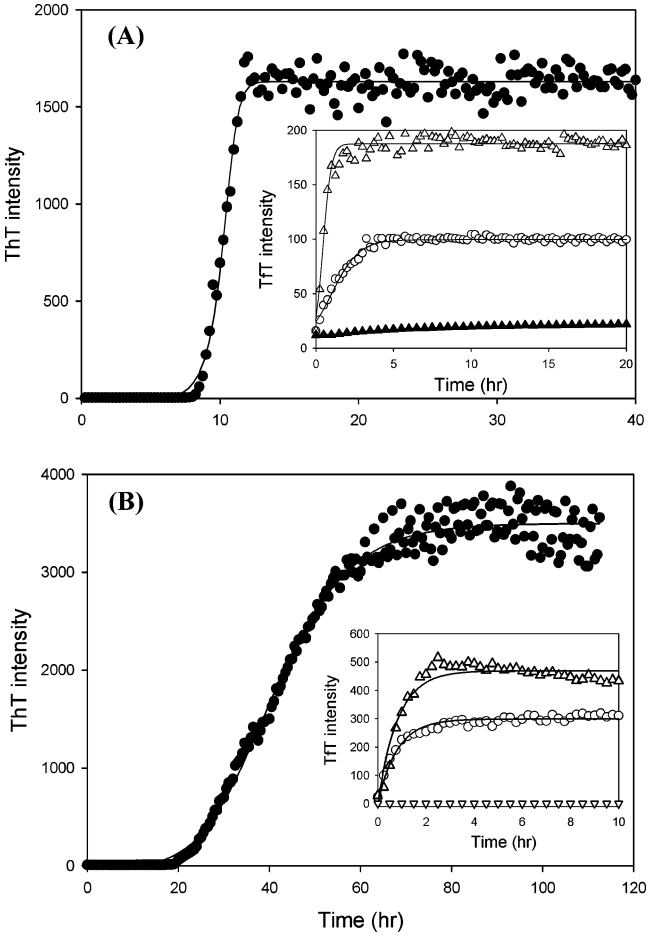

FIGURE 2: Kinetics of fibril formation, monitored by ThT, of human insulin, alkylated A chains, A chain, and B chain. Samples were incubated at 37 °C at (A) pH 1.6 and (B) 7.5: insulin (●), A chain peptide (○), RCAM-Ach (△), RCM-Ach (▽), and B chain peptide (▲). The concentrations of insulin and B chain peptide were 2 and 1 mg/mL, respectively, and the concentrations of A chain and alkylated A chain peptides were 0.5 mg/mL. Note the different ordinate scales in the insets.

RESULTS

Kinetics of Fibrillation of Human Insulin and A and B Chains at Acidic and Neutral pH. The kinetics of formation of amyloid fibrils for insulin and A and B chains were monitored by ThT fluorescence at 37 °C and pH 1.6 and 7.5 (Figure 2). In the case of insulin, the fibrillation shows a pH-dependent lag time, which was much shorter at pH 1.6 (4.5 ± 0.7 h) than at pH 7.5 (23.5 ± 2.1 h). This difference is caused by the fact that low-pH conditions favor the monomer or dimer, whereas the neutral-pH conditions favor the tetramer or hexamer (*31*), and the monomer is required for fibrillation (*40*). On the other hand, the A chain formed amyloid fibrils without a lag phase at both pHs. RCAM-Ach also exhibited a rapid increase in the magnitude of the ThT signal (i.e., no lag) at both pHs. The formation of fibrils by the A chain and RCAM-Ach was confirmed by electron microscopy (Figure 3B−D). The fibrils were straight with a diameter of 10 ± 2 nm and were similar in appearance to insulin fibrils (Figure 3A), except for more lateral association. For RCM-Ach, we observed no increase in the

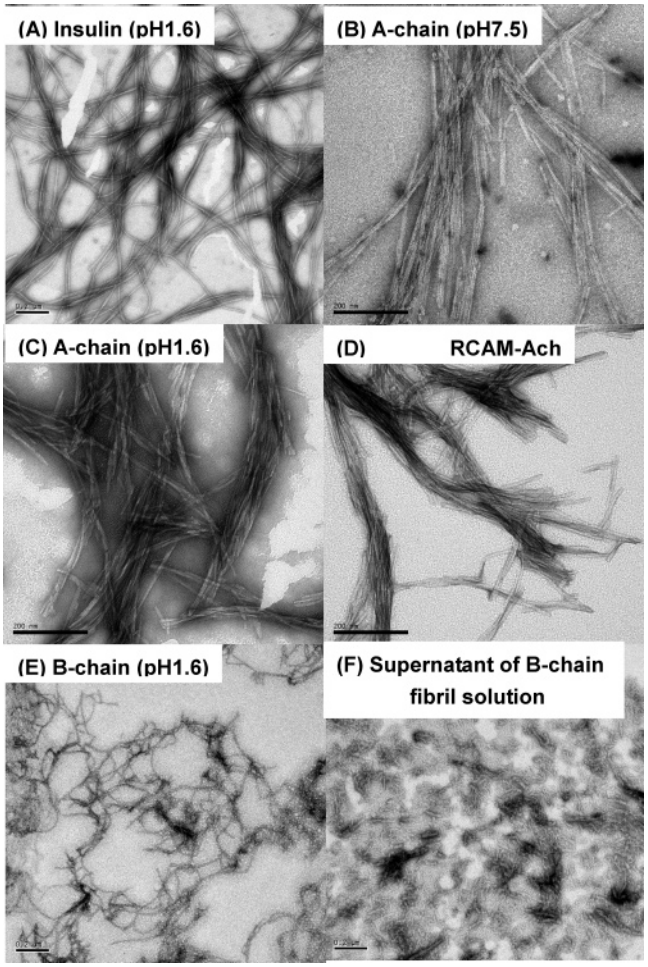

FIGURE 3: Negatively stained transmission electron micrographs of various fibrillar states for human insulin at pH 1.6 (A), A chain at pH 7.5 (B), A chain at pH 1.6 (C), RCAM-Ach at pH 7.5 (D), B chain at pH 1.6 (E), and the supernatant of incubated B chain solutions (F). The scale bar is 200 nm.

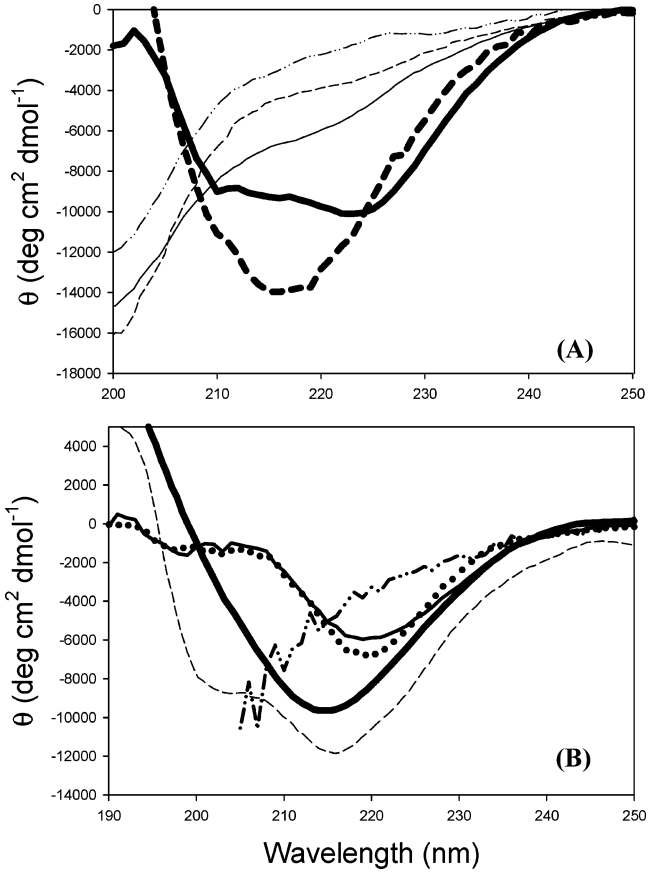

FIGURE 4: Secondary structures of the insulin A and B chains. (A) Far-UV CD spectra at pH 7.5: insulin (thick solid line), A chain (thin solid line), RCAM-Ach (dotted line), RCM-Ach (dotted−dashed line), and fibrils of insulin (thick dotted line). (B) Dependency of CD spectra on the concentration of the B chain: 1 mg/mL (thin solid line), 0.3 mg/mL (thick solid line), 0.1 mg/mL (dashed line), B chain protofilaments (thick dotted line), and 0.1 mg/mL in 5 M GuHCl (dotted−dashed line).

magnitude of the ThT signal (Figure 2B), even after incubation for up to 1 week (data not shown), and no fibrils were observed in the images from EM analysis. This decreased level of self-association is attributed to the change in protein net charge caused by the four added carboxyl groups, resulting in an increased level of electrostatic repulsion between the RCM-Ach peptides, and consequently inhibition of fibrillation.

Intriguingly, the B chain peptide did not exhibit a significant increase in the magnitude of the ThT signal, even after incubation for up to 1 week, in contrast to the A chain. A very small increase in the magnitude of the ThT signal was observed without a lag phase, and EM images showed formation of protofilaments, which were thin (7 ± 2 nm) and very flexible (Figure 3E) in comparison with the insulin and A chain fibrils. In addition, while the mature fibrils of insulin and the A chain were completely removed by centrifugation at 14 000 rpm for 30 min, only 30% of the total B chain peptide was recovered in the pellet under these conditions. The EM images for the supernatant of B chain fibrillation showed the presence of many very short protofilaments reminiscent of those in the incubation mixture and a few very short fibrils (Figure 3F).

Secondary Structure Analysis by Far-UV CD Spectra and B Chain Aggregation. Next, the far-UV CD spectra of human insulin, the A chain, and modified A chains at neutral pH were examined (Figure 4A). The CD spectrum of insulin before fibrillation shows a double minimum at 208 and 222 nm indicative of substantial α-helical structure, consistent with the crystal structure of the insulin hexamer (*32*). We also observed the presence of helical structure at acidic pH (data not shown), which has previously been reported from a NMR solution structure determined under similar conditions of pH but in the presence of 20% acetic acid (*39*). Following incubation at 37 °C with agitation, the CD spectrum assumes a shape that is typical of the presence of β-sheet, characterized by a minimum in the ellipticity at 217 nm, reflecting the large numbers of fibrils that are formed. The CD spectra of the A chain and the alkylated A chains at pH 7.5 exhibited the features of a substantially unfolded conformation although with slight differences between them; e.g., the spectrum of the A chain has some structure with negative ellipticity in the vicinity of 220 nm compared to the alkylated versions. For these A chain peptides, CD spectra were also recorded at pH 1.6 and the same spectral features were observed (data not shown). Comparison of the CD spectra with the fibrillation kinetics shows a correlation between faster fibrillation and less secondary structure in the different forms of the A chain at both acidic and neutral pH, suggesting that less structure in the peptide means that it more readily forms fibrils.

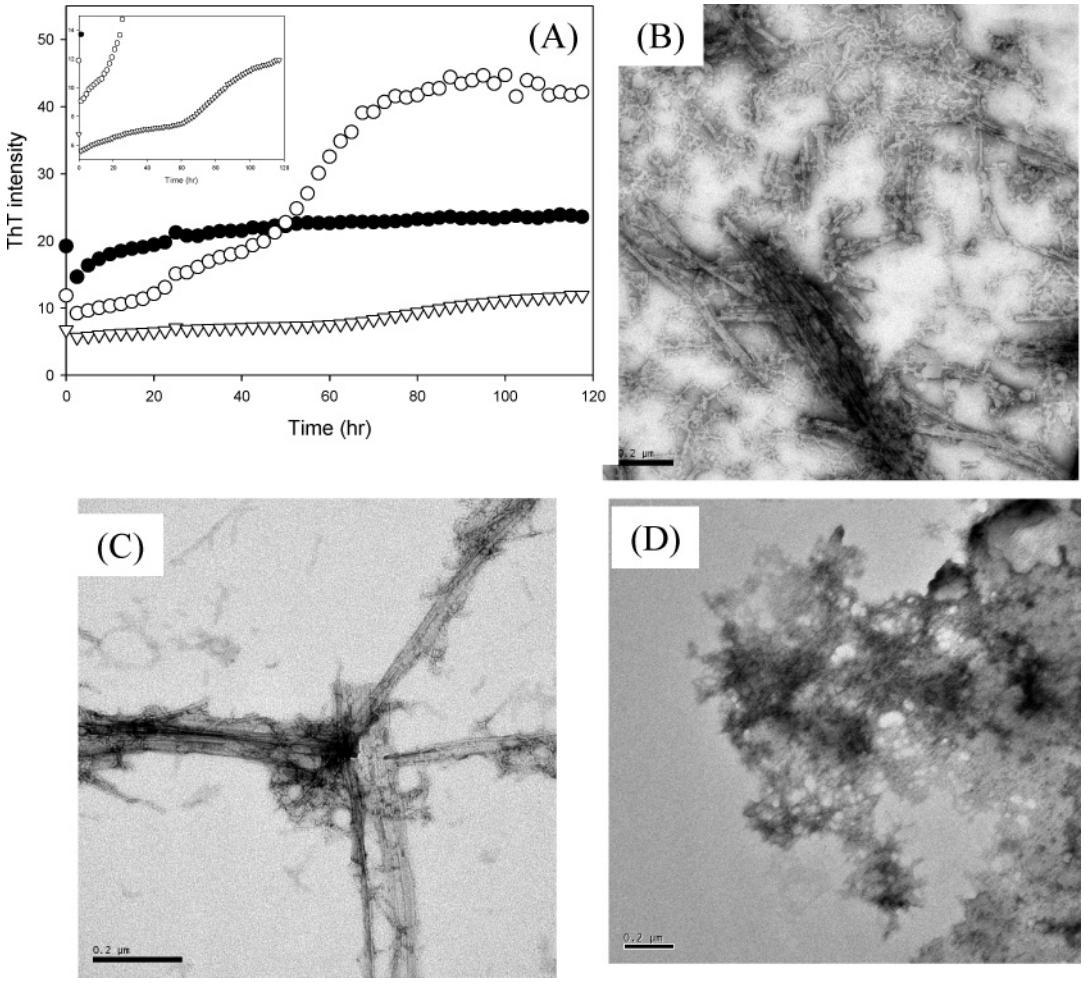

FIGURE 5: Different aggregation states of the insulin B chain. (A) Influence of B chain concentration on its fibril formation monitored by ThT fluorescence. B chain concentrations were 1 (●), 0.5 (○), and 0.2 mg/mL (▽) in 0.025 M HCl and 0.1 M NaCl (pH 1.6), incubated at 37 °C. The inset shows an expanded ordinate view for the fibrillation of 0.2 mg/mL B chain, showing the two transitions, as seen at 0.5 mg/mL. Corresponding EM images for 0.5 (B) and 0.2 mg/mL (C) fibrillated B chain. (D) EM image of soluble aggregates of B chain insulin.

In contrast, the CD spectrum of the B chain at pH 1.6 prior to incubation at 37 °C shows β-sheet conformation with a negative peak at 217 nm, which is dependent on the B chain concentration (Figure 4B), indicating formation of soluble oligomers (confirmed by EM; see Figure 5D). The spectrum of B chains at a low concentration (0.1 mg/mL) shows two minima in the 216−217 and 200−202 nm regions, diagnostic of coexisting β-sheet and unfolded structures. In the presence of 5 M GuHCl, however, the spectrum indicates a completely denatured structure. Interestingly, the spectrum of the protofilaments of the B chain also shows a typical β-sheet rich conformation with the negative peak at 217 nm, and almost the same spectrum as the one before the incubation and/or fibrillation, suggesting that there is no significant change in the amount of β-structure in going from the B chain soluble oligomers to the protofilaments. Though the far-UV CD spectrum of mature fibrils of insulin was similar to that of the B chain protofilaments, the negative intensity of the fibrils was larger than that of protofilaments, suggesting structural differences between the mature fibrils and protofilaments. As discussed subsequently, the B chain protofilaments do not appear to be intermediates on the pathway to mature fibrils.

Effect of B Chain Concentration on Fibrillation. In view of the concentration-dependent CD spectra, we examined the effect of the concentration of the B chain on its fibrillation at acidic pH (Figure 5). The kinetics of B chain fibrillation were markedly dependent on peptide concentration. For example, incubation of 0.2 mg/mL B chain showed a long lag time (65 ± 9 h), whereas the lag time of 0.5 mg/mL B chain was much shorter (30 ± 4 h). At higher concentrations such as 1.0 mg/mL, however, there was no lag time, and only a small increase in ThT intensity was observed. From EM analysis, we observed mature fibrils for 0.5 mg/mL B chain, as well as protofilaments (Figure 5 B), consistent with the idea that low concentrations of the B chain lead to dissociation of the soluble oligomers to provide monomers that can form mature amyloid fibrils of the B chain. The EM image for 0.2 mg/mL B chain shows some protofilaments but mostly mature fibrils (Figure 5C). These observations can be explained as follows (Scheme 1). At low B chain concentrations, there will be more monomer and less soluble aggregate. The monomers can associate and form mature fibrils with typical fibrillation kinetics (i.e., a lag followed by exponential growth). However, at higher concentrations, the B chains are present as the soluble oligomers and these rapidly and preferentially form protofilaments and not mature fibrils.

Actually, the kinetics for fibrillation at 0.2 and 0.5 mg/mL B chain are more complex then the typical sigmoidal

Scheme 1

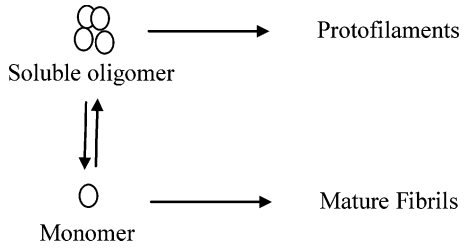

curve defined by an initial lag phase, a subsequent growth phase, and a final equilibrium phase; instead, the traces appear to be composed of two transitions, an initial one due to the formation of protofilaments and a second larger increase in ThT intensity due to formation of mature fibrils (e.g., see the inset of Figure 5A). Our results clearly show that B chain fibrillation has a lag phase for mature amyloid fibril formation in contrast to the results of the A chain fibrillation and B chain protofilament formation in which there is no lag phase.

Effect of GuHCl on B Chain Fibrillation. Denaturants are known to decrease the level of association of aggregated polypeptides, so we next investigated the effects of GuHCl on B chain fibrillation, with the expectation that low concentrations of denaturant would increase the amount of monomeric B chain at higher concentrations of the peptide and, hence, according to our hypothesis, increase the level of formation of mature fibrils. This was confirmed using light scattering, which showed a sharp drop in aggregate size going from 0 to 0.5 M GdnHCl, attributed to dissociation of the soluble oligomers into monomers, followed by a small increase at higher denaturant concentrations, presumably reflecting unfolding of the monomer. The kinetics of 1 mg/mL B chain incubated at pH 1.6 and 37 °C in the presence of GuHCl, monitored by ThT fluorescence, are shown in Figure 6. We observed the typical sigmoidal curves of the ThT signal at low concentrations of GuHCl (0.3−1.0 M). The kinetic curves show an initial lag phase, an exponential growth phase, and a final equilibrium phase with a strong ThT signal; this is in contrast to the absence of GuHCl, in which no lag was seen and much lower ThT intensities were observed (Figure 5A), and suggests a different mechanism of fibrillation in the presence of the denaturant. At higher GuHCl concentrations, the peptide becomes denatured and no fibrils are formed.

Figure 6B shows the lag times calculated from curve fitting as a function of GuHCl concentration. The lag time decreased with an increase in GuHCl concentration to a minimum at 0.7 M GuHCl and then increased at higher concentrations. The final ThT signals have also been monitored as a function of GuHCl concentration in Figure 6B. These show a maximum value at ∼0.5−0.7 M GuHCl, which is consistent with the region of GuHCl concentration accelerating the B chain fibrillation, and we observed the most fibrils in the pellet after centrifugation in this region of GuHCl concentration (Figure 6C), suggesting that very low concentrations of GuHCl increase the rate of B chain fibrillation as well as the amount of mature fibrils that is formed.

EM pictures of B- hain fibrils grown in the presence of GuHCl at pH 1.6 are shown in Figure 7. In the presence of 0.1 or 0.2 M GuHCl, the EM images showed mixtures of short protofilaments and mature fibrils (Figure 7A,B). At

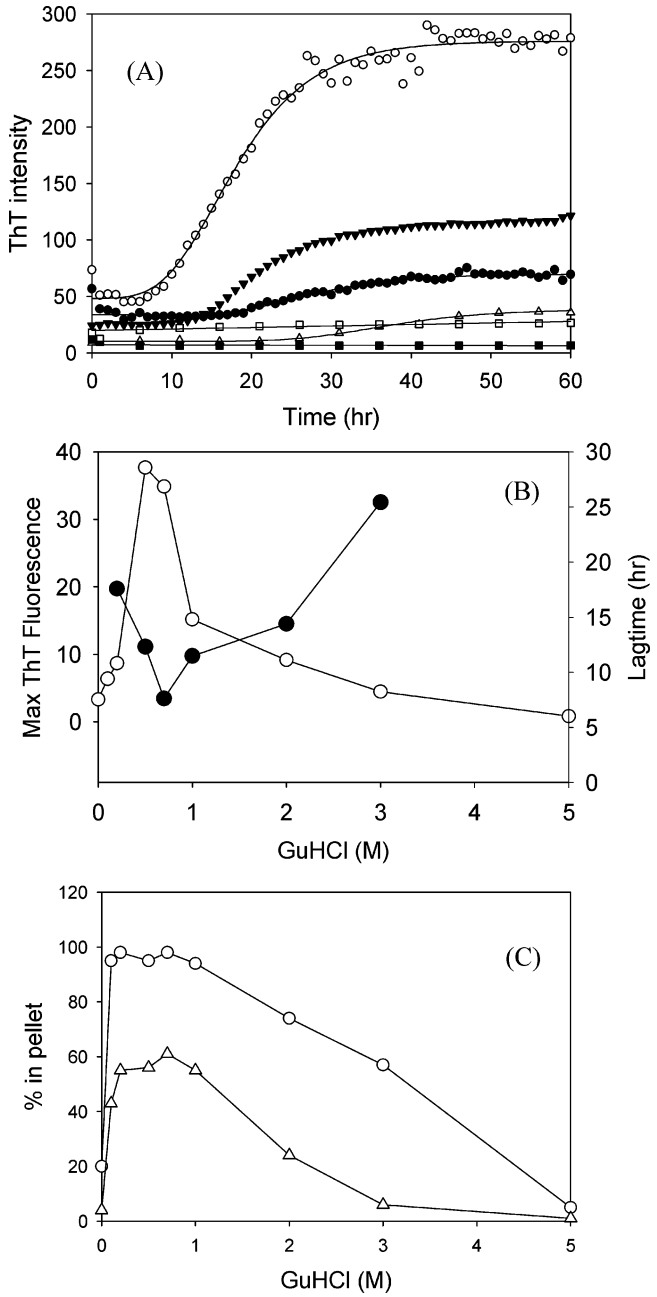

FIGURE 6: Effects of GuHCl on the fibrillation of B chain insulin. (A) Kinetics of B chain (1 mg/mL) fibrillation at pH 1.6 monitored by ThT fluorescence: 0 (control) (□), 0.2 (●), 0.7 (○), 1 (▼), 3 (△), and 5 M GuHCl (■). (B) Dependencies of the lag time (○) and final ThT fluorescence (60 h) (●) on GuHCl concentration. (C) Amount of protein (○) and ThT (△) in the pellet after incubation in the presence of GuHCl.

GuHCl concentrations of 0.5 or 0.7 M, however, the EM images show mature fibrils with extensive lateral association (Figure 7C,D), with a diameter of 10 ± 2 nm, similar to insulin fibrils, and B chain fibrils grown at low protein concentrations in the absence of GuHCl. When the incubation mixtures of the mature fibrils of the B chain formed in low concentrations of GuHCl were centrifuged, all the protein was in the pellet, suggesting that under these conditions essentially all of the B chain molecules formed mature fibrils, since protofilaments were not significantly removed by such a centrifugation (see above). In high concentrations of GuHCl, where incubation of the B chain gave weak ThT signals, the EM images showed more short and clumped

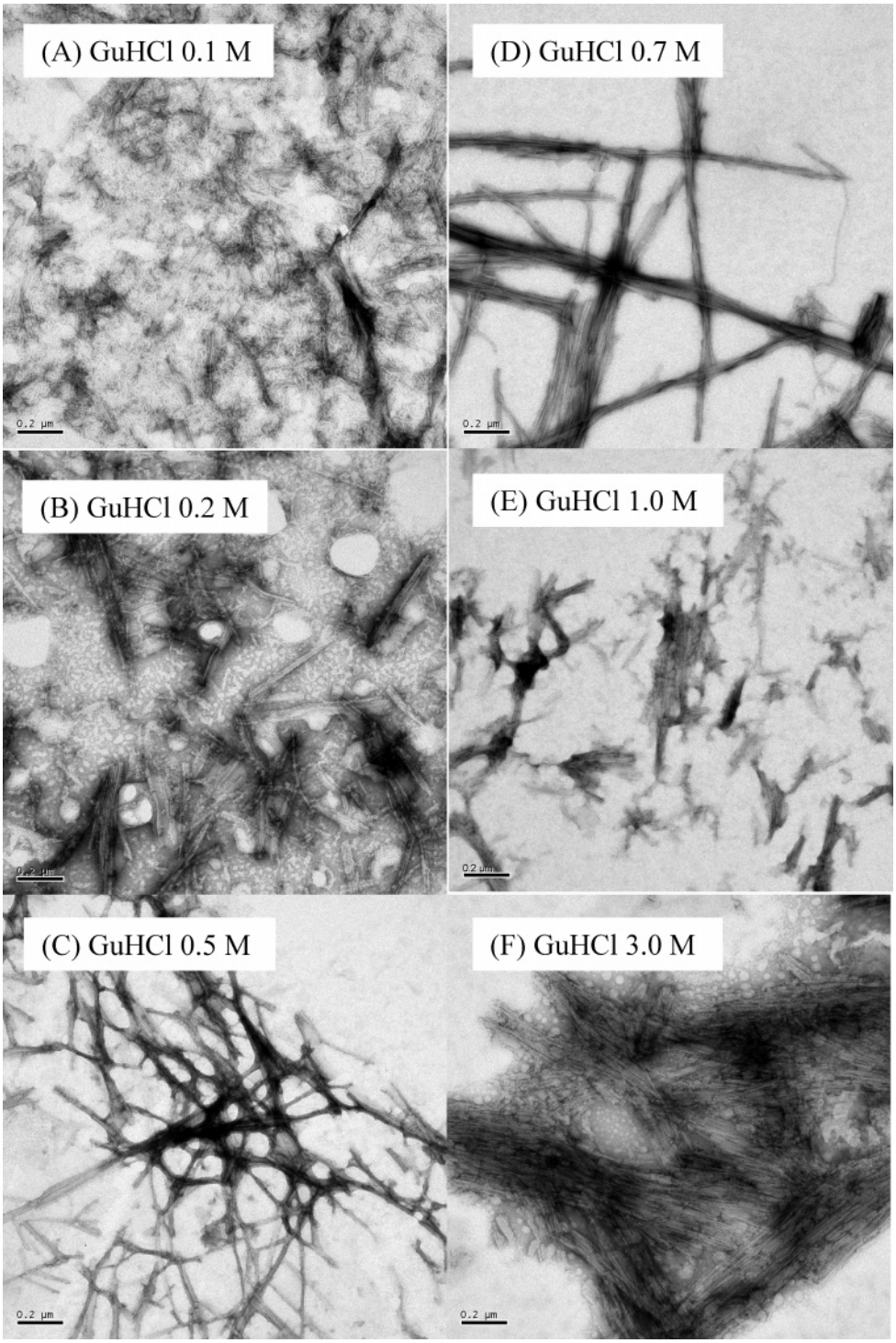

FIGURE 7: Electron micrograph images of B chain fibrils. The images show the morphology of fibrils at various GuHCl concentrations at pH 1.6: (A) 0.1, (B) 0.2, (C) 0.5, (D) 0.7, (E) 1.0, and (F) 3 M GuHCl. The scale bar is 200 nm.

fibrils than in low concentrations of GuHCl (Figure 7E,F). These results are consistent with EM images of insulin fibrils in high concentrations of GuHCl (*40*).

We interpret these results to mean that low concentrations of GuHCl, optimally around 0.7 M, dissociate the soluble oligomers of the B chain peptide to form monomeric species which undergo "normal" fibrillation to form mature fibrils. At >1 M GuHCl, denaturation of these monomers becomes increasingly predominant, so fewer fibrils are formed.

Effect of GuHCl on the Structure of the B Chain. Low concentrations of GuHCl have been shown to dissociate insulin hexamers into dimers or monomers and partially unfolded states that lead to accelerated fibrillation (*40*). To confirm that the acceleration of B chain fibrillation in the presence of GuHCl is due to the induction of a monomeric amyloidogenic intermediate due in turn to dissociation of the soluble B chain oligomers, we analyzed the CD and ANS binding properties of the B chain. Figure 8 shows the far-UV CD spectra of the B chain in the presence of various concentrations of GuHCl. These experiments were carried out at 1 mg/mL B chain, the same concentration as in the fibrillation experiments. At low concentrations of GuHCl,

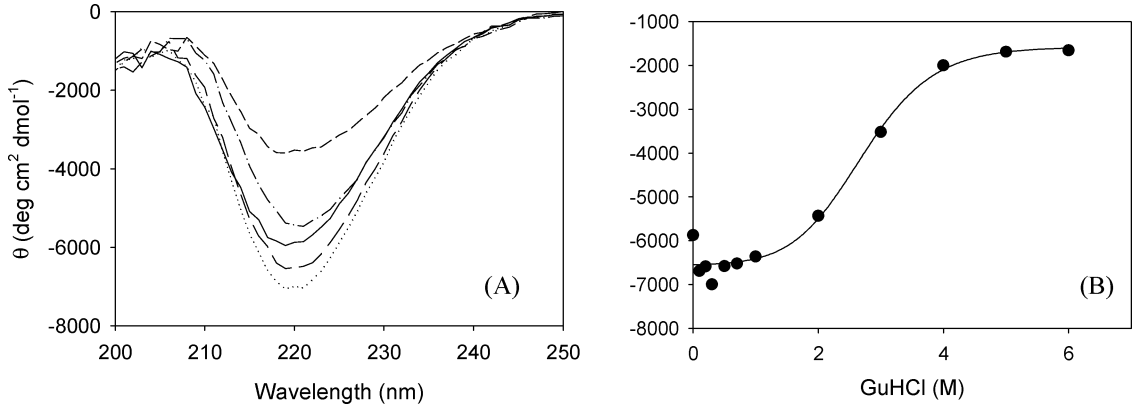

FIGURE 8: Effect of GuHCl on the structure of the insulin B chain (1 mg/mL), monitored by circular dichroism at pH 1.6: (A) far-UV CD spectra and (B) GuHCl dependency of the ellipticity at 220 nm.

the spectrum of the B chain exhibited substantial β-sheet structure, the amount of which decreased at >2 M GuHCl. The ellipticities at 220 nm were plotted against the concentration of GuHCl in Figure 8B. The negative ellipticity increased initially to a minimum at 0.3 M GuHCl, paralleling the effects of GuHCl on the fibrillation kinetics of the B chain peptide (Figure 6B), consistent with the idea that dissociation of soluble oligomers is required for mature fibril formation. The spectra changed markedly above 2 M GuHCl, presumably reflecting denaturation of the peptide.

We also examined the effects of GuHCl on the binding of ANS to the B chain to obtain further information about the peptide conformation (Figure 9). Hydrophobic ligands such as ANS and bis-ANS bind to hydrophobic regions of partially folded intermediates (*41*−*45*), resulting in a marked increase in fluorescence emission of the ANS ligands and a change in λ_{max}. The fluorescence emission spectra of ANS in the presence of the B chain are shown in Figure 9A. Interestingly, ANS binds strongly to the B chain in the absence of GuHCl at pH 1.6, while it does not bind to insulin under these conditions, suggesting that the B chain peptide is partially folded and/or that it forms oligomers that have hydrophobic binding sites for ANS. The ANS fluorescence intensities at 480 nm for the B chain and insulin are plotted versus the GuHCl concentration in Figure 9B. The changes in fluorescence intensity for insulin show unfolding induced by GuHCl with a partially folded intermediate at ~1.0 M GuHCl; in contrast, the fluorescence for the B chain essentially decreases monotonically with an increase in GuHCl concentration. The corresponding effects on the λ_{max} of ANS binding are shown in Figure 9C and show essentially no change as a function of GuHCl concentration. These observations suggest that the B chain molecules in the oligomers are already partially unfolded and become even less structured as the GuHCl concentration increases above 0.5 M.

From these results, we can account for the formation of mature fibrils of the B chain in the presence of low concentrations of GuHCl by the dissociation of soluble B chain oligomers, as shown in the model of Scheme 1, and indicating that the initial association state is an important factor in determining the type of fibrillar material formed by the B chain. Figure 6C shows that the amount of total protein spun down in the pellet (essentially the amount of mature B chain fibrils formed) reaches a maximum at very low GuHCl concentrations and then slowly decreases with an increase in GuHCl concentration, again consistent with low denaturant concentrations leading to dissociation of soluble oligomers and formation of mature B chain fibrils.

Role of B Chain Protofilaments. We then investigated whether B chain protofilaments could convert into mature fibrils, since protofilaments are usually intermediates on the pathway to mature fibrils in most amyloid fibril systems. The kinetics of protofilament formation were compared with the kinetics of the extension reaction of the mature fibrils by the addition of seed fibrils (Figure 10). After incubation under conditions in which the B chain forms protofilaments, the final ThT intensity has a low value of 30; however, the addition of B chain seed fibrils (formed in 0.7 M GuHCl) at the start of the incubation leads to the formation of mature B chain fibrils with a ThT intensity of 150, 5 times higher than that of protofilaments at the same concentration. This intensity is still lower than the value of 250 for B chain mature fibrils formed directly in 0.7 M GuHCl (Figure 6A). EM images after incubation of the B chain in which seeds were added at time zero show the existence of laterally associated mature fibrils with a background of protofilaments (Figure 10B), suggesting that the high ThT intensity is due to the formation of mature fibrils of the B chain. These results (along with those of Figure 5) indicate that the fluorescence of ThT bound to the protofilaments is much lower than that of the mature amyloid fibrils and that the majority of the protofilaments do not convert into the mature fibrils even after the addition of seed fibrils. After the incubation, we measured the amount of protein in the pellet and found 50−70% of the total protein, indicating that 30−50% of the protein still remains in the supernatant (as protofilaments and/or soluble oligomers), presumably due to the lack of dissociation of soluble oligomers preventing mature fibril formation.

We also examined whether the protofilaments can be converted into mature fibrils by adding seeds of mature fibrils after incubation of the B chain for 45 h (Figure 10A). Interestingly, a small increase in the magnitude of the ThT signal was noted, to a value of 100. This increase is attributed to the formation of B chain mature fibrils, probably from the small amount of monomer present. When we analyzed this sample with EM, a mixture of mature fibrils and protofilaments was observed (Figure 10C), with a much higher fraction of protofilaments compared to the sample seeded at time zero (Figure 10B). The amount of protein in the pellet was 30−50% of the total protein, suggesting that

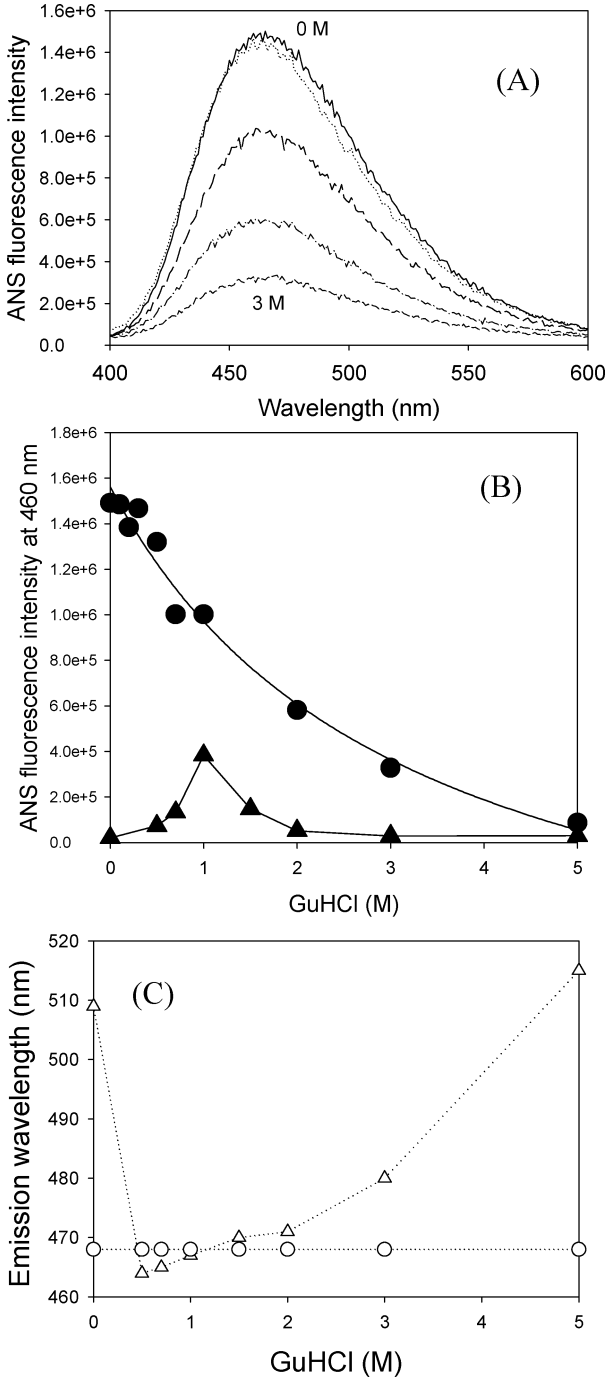

FIGURE 9: Effect of GuHCl on ANS binding of the B chain peptide, at pH 1.6. (A) ANS fluorescence emission spectra of a B chain (1 mg/mL) solution containing 10 μM ANS with various GuHCl concentrations: 0 (—), 0.3 (•••), 0.7 (– – –), 2.0 (–•–), and 3.0 M (- - -). (B) GuHCl dependency of ANS fluorescence intensities at 460 nm for B chain (●) and monomeric insulin (▲). (C) GuHCl dependency of the emission wavelength for B chain (○) and monomeric insulin (△).

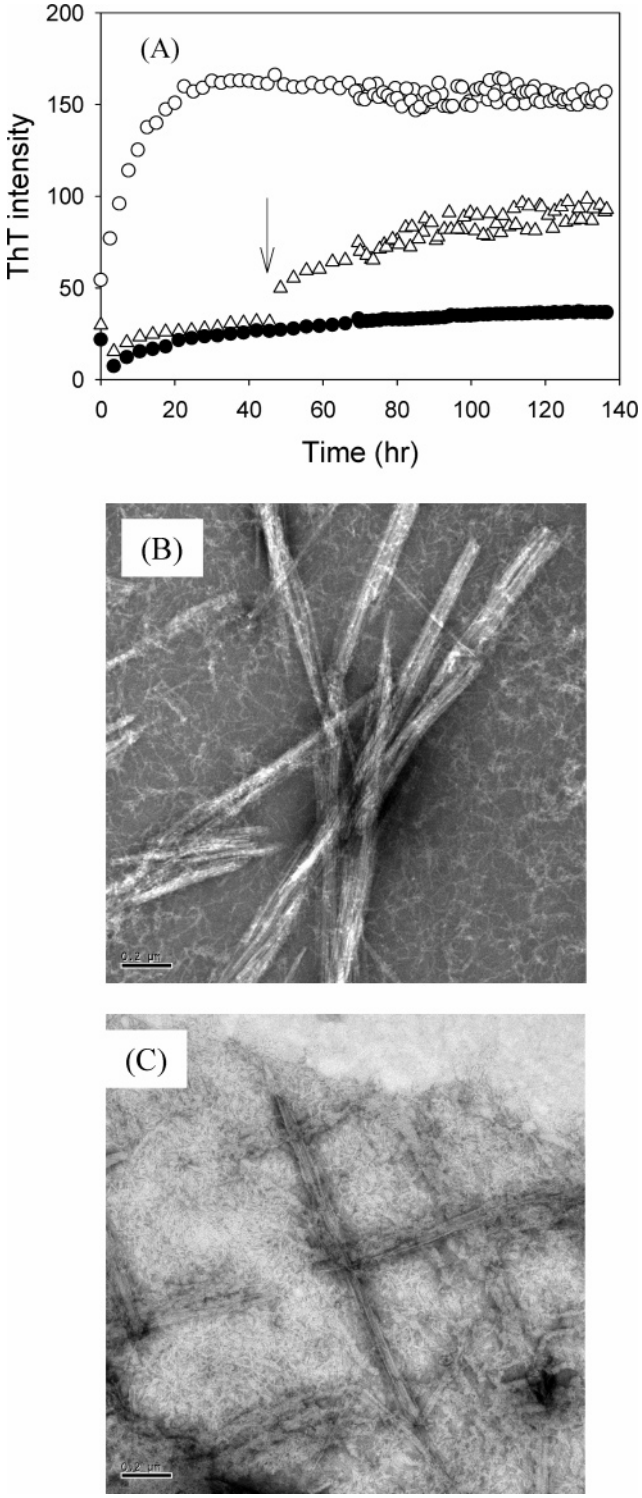

FIGURE 10: Effect of seeding on B chain fibrillation. (A) Seeding effect on the kinetics of B chain fibrillation monitored with ThT. Seed fibrils of the B chain (0.1 mg/mL), formed in the presence of 0.7 M GuHCl, were added to the B chain solution 0 (○) and 45 h (△) after incubation (arrow). The filled circles show the corresponding curve in the absence of seeding. (B) EM images of B chain fibrils formed in the presence of seed fibrils added at the beginning of the incubation and (C) after incubation for 45 h.

the protofilaments could not convert into the mature fibrils. On the basis of these observations, we conclude that the B chain protofilaments are not intermediates on the pathway to mature amyloid fibrils but an off-pathway or dead-end product.

DISCUSSION

Roles of A and B Chains in the Fibrillation of Insulin. It has been proposed that insulin fibrillation occurs through the dissociation of the native oligomers into the monomer; the monomer then undergoes a structural change to a partially folded intermediate, which has a strong propensity for fibrillation (*28*, *30*, *40*, *46*−*48*). For this reason, the fibrillation of insulin at acidic pH (conditions favoring monomer

and/or dimer) occurs more readily than that at neutral pH (conditions favoring tetramer and/or hexamer). It is known that short peptides including key amyloidogenic residues of larger proteins can form amyloid fibrils. Thus, the fact that the fibrillation of the insulin A chain occurred easily with no lag phase in a pH-independent manner could indicate that the A chain may be, or include, the key sequence for insulin fibrillation. The observation that fibrils of both the A chain and the alkylated A chain with iodoacetamide (RCAM-Ach) exhibited the same morphology and similar kinetics of formation indicates that the cysteine residues do not play a critical role in fibrillation. In contrast, the lack of fibrillation by the A chain alkylated with iodoacetic acid (RCM-Ach), presumably due to the increase in the level of electrostatic repulsion, demonstrates the critical nature of small changes in the nature of residues not necessarily involved directly in self-association in the formation of amyloid fibrils.

Unlike the A chain peptide, which is quite soluble, the B chain forms insoluble aggregates at neutral pH and soluble oligomers at acidic pH. This suggests that the B chain peptide has a stronger intrinsic propensity to self-associate than the A chain. Interestingly, the B chain did not form typical mature amyloid fibrils except at very low concentrations, where significant amounts of monomer were present. Instead, the soluble oligomers lead to the formation of protofilaments. The driving force for insulin aggregation is assumed to be hydrophobic in nature, and it has been suggested that the initial step in aggregation is probably the formation of monomeric, partially folded molecules, in which hydrophobic faces, normally buried in the dimer and hexamer, become exposed to solvent (*33*, *47*). Most amino acid residues in the B chain are involved in either dimer or hexamer insulin formation (Figure 1A), and these hydrophobic properties of the B chain are considered to be a driving force for insulin aggregation when they become exposed to solvent by the dissociation of the dimer or hexamer into the monomer. Thus, the facile association of the B chain to form soluble oligomers at neutral pH near its pI is not unexpected. At acidic pH, however, although the B chain peptide is soluble, it is mostly present as oligomers that lead to formation of protofilaments with no lag phase (Figure 2A).

One of the unusual aspects of A chain fibrillation is the significant amount of lateral association of fibrils formed from the A chain: this could reflect a tendency for nucleation on the side of existing fibrils or a strong lateral interaction between fibrils due the exposure of either hydrophobic or electrostatic (or both) interactions of residues on the surface of the fibril.

Protofilaments and Fibrils of Insulin B Chains. For insulin B chains, the protofilaments are thin and very flexible fibers with low ThT intensity, and the mature fibrils are straight and thicker with high ThT intensity and also possess a strong tendency to associate laterally. Protofibrils are usually considered as a transient species during formation of mature amyloid fibrils and have been implicated in the toxicity responsible for cell dysfunction and neuronal loss in Alzheimer's disease and other protein aggregation diseases (*49*−*51*). However, it is not always clear whether protofibrils are on the fibrillation pathway. Our results indicate that protofilaments of the B chain do not readily convert into mature amyloid fibrils, suggesting that the protofilaments might be an off-pathway product. Similar results have been shown from β2-microglobulin, a major component of dialysis-related amyloid fibrils (*52*): thin and flexible protofilaments of β2-microglobulin, prepared under conditions of high salt at acidic pH, had no seed function and a weak ThT signal and did not convert into mature fibrils. Protofilaments were also observed to form at a slow rate spontaneously, analogous to the situation with insulin (Figures 2 and 5). Since fibril formation occurs very rapidly once nucleation is complete, the slow rate of protofilament formation observed with the B chains might be an inherent property of dead-end protofilaments.

Fibrillation of the B Chain Depends on Its Association State. One of the most interesting findings from this investigation is that B chain fibrillation is affected by the nature of the soluble oligomers. Freshly prepared B chains from the reduction of insulin are aggregated at neutral pH, in the vicinity of its pI (Figure 1B). At acidic pH, while they are apparently soluble, B chains nevertheless still form a soluble aggregate except at very low protein concentrations. Since low concentrations of the B chain can form mature amyloid fibrils with a typical lag phase, we assume that this reflects the properties of the monomeric form of the B chain. However, higher concentrations of the B chain lead to a combination of soluble oligomers and protofilaments. Thus, the ability to form fibrils is affected by the association state of the starting material. One possible explanation for this is that the soluble oligomers directly interact to form protofilaments without proceeding through a monomeric species.

The addition of GuHCl markedly affects B chain fibrillation. We attribute the effects of low concentrations of GuHCl predominantly to dissociation of soluble oligomers into monomers. We believe that these monomers are partially unfolded, permitting the necessary topological rearrangements of the polypeptide for formation of the β-sheet structure of the fibril.

Our results demonstrate that mature B chain fibrils are formed only from monomers, which are only found significantly at low B chain concentrations (<0.2 mg/mL) or in the presence of low concentrations of GuHCl with higher concentrations of the B chain, whereas protofilaments form directly from the soluble oligomers, without formation of a critical nucleus (hence, the lack of a lag phase). The fact that they do not go on to form mature fibrils suggests that the underlying structure of the protofilaments must have some critical differences from mature fibrils.

In conclusion, the three major findings from this study are first that both insulin A and B chains can form fibrils, suggesting that regions of both chains are involved in the self-association leading to insulin fibrillation. Second, the data indicate that the association state of the starting species can have dramatic effects on the final product of aggregation and fibrillation. Third, a specific polypeptide, in this case B chain insulin, can form two very different types of non-interconverting fibrils, namely, the protofilaments and the mature fibrils.

REFERENCES

1. Buxbaum, J. N. (2004) The systemic amyloidoses, *Curr. Opin. Rheumatol. 16*, 67−75.
2. Fink, A. L. (1997) Protein aggregation: Folding aggregates, inclusion bodies and amyloid, *Folding Des. 3*, R9−R23.

3. Dobson, C. M. (1999) Protein misfolding, evolution and disease, *Trends Biochem. Sci. 24*, 329−332.
4. Chiti, F., Webster, P., Taddei, N., Clark, A., Stefani, M., Ramponi, G., and Dobson, C. M. (1999) Designing conditions for in vitro formation of amyloid protofilaments and fibrils, *Proc. Natl. Acad. Sci. U.S.A. 96*, 3590−3594.
5. Fandrich, M., Fletcher, M. A., and Dobson, C. M. (2001) Amyloid fibrils from muscle myoglobin, *Nature 410*, 165−166.
6. Hamada, D., and Dobson, C. M. (2002) A kinetic study of β-lactoglobulin amyloid fibril formation promoted by urea, *Protein Sci. 11*, 2417−2426.
7. MacPhee, C. E., and Dobson, C. E. (2000) Chemical dissection and reassembly of amyloid fibrils formed by a peptide fragment of transthyretin, *J. Mol. Biol. 297*, 1203−1225.
8. Höggovist, B., Näslund, J., Sletten, K., Westermark, G. T., Mucchiano, G., Tjernberg, L. O., Nordstedt, C., Engström, U., and Westermark, P. (1999) Medin: An integral fragment of aortic smooth muscle cell-produced lactadherin forms the most common human amyloid, *Proc. Natl. Acad. Sci. U.S.A. 96*, 8669−8674.
9. Serpell, L. C. (2000) Alzheimer's amyloid fibrils: Structure and assembly, *Biochim. Biophys. Acta 1502*, 16−30.
10. Balbach, J. J., Ishii, Y., Antzutkin, O. N., Leapman, R. D., Rizzo, N. W., Dyda, F., Reed, J., and Tycko, R. (2000) Amyloid Fibril Formation by Aβ_{16-22}, a Seven-Residue Fragment of the Alzheimer's β-Amyloid Peptide, and Structural Characterization by Solid State NMR, *Biochemistry 39*, 13748−13759.
11. Kozhukh, G. V., Hagihara, Y., Kawakami, T., Hasegawa, K., Naiki, H., and Goto, Y. (2002**)** Investigation of a Peptide Responsible for Amyloid Fibril Formation of β_2-Microglobulin by *Achromobacter* Protease I, *J. Biol. Chem. 277*, 1310−1315.
12. Uversky, V. N., Li, J., and Fink, A. L. (2001) Pesticides directly accelerate the rate of α-synuclein fibril formation: A possible factor in Parkinson's disease, *FEBS Lett. 500*, 105−108.
13. Uversky, V. N., Cooper, E. M., Bower, K. S., Li, J., and Fink, A. L. (2002) Accelerated α-synuclein fibrillation in crowed milieu, *FEBS Lett. 515*, 99−103.
14. Cohlberg, J. A., Li, J., Uversky, V. N., and Fink, A. L. (2002**)** Heparin and Other Glycosaminoglycans Stimulate the Formation of Amyloid Fibrils from α-Synuclein in Vitro, *Biochemistry 41*, 1502−1511.
15. Walsh, D. M., Lomakin, A., Benedek, G. B., Condron, M. M., and Teplow, D. B. (1997) Amyloid β-protein fibrillogenesis: Detection of a protofibrillar intermediate, *J. Biol. Chem. 272*, 22364−22372.
16. Walsh, D. M., Hartley, D. M., Kusumoto, Y., Fezoui, Y., Condron, M. M., Lomakin, A., Benedek, G. B., Selkoe, D. J., and Teplow, D. B. (1999) Amyloid β-protein fibrillogenesis: Structure and biological activity of protofibrillar intermediates, *J. Biol. Chem. 274*, 25945−25952.
17. Jiang, Y., Li, H., Zhu, L., Zhou, J.-M., and Perrett, S. (2004) Amyloid nucleation and hierarchical assembly of Ure2p fibrils, *J. Biol. Chem. 279*, 3361−3369.
18. Tycko, R. (2004) Progress towards a molecular-level structural understanding of amyloid fibrils, *Curr. Opin. Struct. Biol. 14*, 96−103.
19. Sunde, M., and Blake, C. F. (1997) The structure of amyloid fibrils by electron microscopy and X-ray diffraction, *Adv. Protein Chem. 50*, 123−159.
20. Serpell, L. C., and Smith, J. M. (2000) Direct visualization of the β-sheet structure of synthetic Alzheimer's amyloid, *J. Mol. Biol. 299*, 225−231.
21. Petkova, A. T., Ishii, Y., Balbach, J. J., Antzutkin, O. N., Leapman, R. D., Delaglio, F., and Tycho, R. (2002) A structural model for Alzheimer's β-amyloid fibrils based on experimental constraints from solid-state NMR, *Proc. Natl. Acad. Sci. U.S.A. 99*, 16742−16747.
22. Zurdo, J., Guijarro, J. I., and Dobson, C. M. (2001) Preparation and characterization of purified amyloid fibrils, *J. Am. Chem. Soc. 123*, 8141−8142.
23. Kheterpa, I., Zhou, S., Cook, K. D., and Wetzel, R. (2000**)** Aβ amyloid fibrils possess a core structure highly resistant to hydrogen exchange, *Proc. Natl. Acad. Sci. U.S.A. 97*, 13597−13601.
24. Hoshino, M., Katou, H., Hagihara, Y., Hasegawa, K., Naiki, H., and Goto, Y. (2002) Mapping the core of the β_2-microglobulin amyloid fibril by H/D exchange, *Nat. Struct. Biol. 9*, 332−336.
25. Waugh, D. F. (1946) A fibrous modification of insulin. I. The heat precipitate of insulin, *J. Am. Chem. Soc. 68*, 247−250.
26. Waugh, D. F., Wilhelmson, D. F., Sackler, M. L., and Commerford, S. L. (1953) Studies of the Nucleation and Growth Reactions of Selected Types of Insulin Fibrils *J. Am. Chem. Soc. 75*, 2592−2600.
27. Blundell, T. L., Dodson, G. G., Hodgkin, D. M., and Merola, D. (1972) Insulin, *Adv. Protein Chem. 26*, 279−402.
28. Nielsen, L., Khurana, R., Coats, A., Frokjaer, S., Brange, J., Vyas, S., Uversky, V., and Fink, A. L. (2001) Effect of environmental factors on the kinetics of insulin fibril formation: Elucidation of the molecular mechanism, *Biochemistry 40*, 6036−6046.
29. Ahmad, A., Uversky, V. N., Hong, D., and Fink, A. L. (2005) Early events in the fibrillation of monomeric insulin, *J. Biol. Chem 280*, 42669−42675.
30. Brange, J., Andersen, L., Laursen, E. D., Meyn, G., and Rasmussen, E. (1997) Toward understanding insulin fibrillation, *J. Pharm. Sci. 86*, 517−525.
31. Brange, J., Skelbaek-Pedersen, B., Langkjaer, L., Damgaard, U., Ege, H., Havelund, S., Heding, L. G., Jorgensen, K. H., Lykkeberg, J., Markussen, J., Pingel, M., and Rasmussen, E. (1987) *Galenics of Insulin. The physicochemical and pharmaceutical aspects of insulin and insulin preparations*, Springer-Verlag, Berlin.
32. Blundell, T. L., Cutfield, J. F., Cutfield, S. M., Dodson, G., Dodson, G. G., Hodgkin, D. C., Mercola, D. A., and Vijayan, M. (1971) Atomic Positions in Rhombohedral 2-Zinc Insulin Crystals, *Nature 231*, 506−511.
33. Nielsen, L., Frokjaer, S., Brange, J., Uversky, V. N., and Fink, A. L. (2001) Probing the Mechanism of Insulin Fibril Formation with Insulin Mutants, *Biochemistry 40*, 8397−8409.
34. Jimenez, J. L., Nettleton, E. J., Bouchard, M., Robinson, C. V., Dobson, C. M., and Saibil, H. R. (2002) The protofilament structure of insulin amyloid fibrils, *Proc. Natl. Acad. Sci U.S.A. 99*, 9196−9201.
35. Hua, Q. X., and Weiss, M. A. (2004) Mechanism of insulin fibrillation: The structure of insulin under amyloidogenic conditions resembles a protein-folding intermediate, *J. Biol. Chem. 279*, 21449−21460.
36. Knegtel, R. M., Boelens, R., Ganadu, M. L., and Kaptein, R. (1991) The solution structure of a monomeric insulin. A two-dimensional ^{1}H NMR study of des-(B26−B30)-insulin in combination with distance geometry and restrained molecular dynamics, *Eur. J. Biochem. 202*, 447−458.
37. Whittingham, J. L., Scott, D. J., Chance, K., Wilson, A., Finch, J., Brange, J., and Dodson, G. G. (2002) Insulin at pH 2: Structural analysis of the conditions promoting insulin fibre formation, *J. Mol. Biol. 318*, 479−490.
38. Panse, V. G., Vogel, P., Trommer, W. E., and Varadarajan, R. (2000**)** A Thermodynamic Coupling Mechanism for the Disaggregation of a Model Peptide Substrate by Chaperone SecB, *J. Biol. Chem. 275*, 18698−18703.
39. Hua, Q., and Weiss, M. A. (1991) Comparative 2D NMR studies of human insulin and des-pentapeptide insulin: Sequential resonance assignment and implications for protein dynamics and receptor recognition, *Biochemistry 30*, 5505−5515.
40. Ahmad, A., Millett, I. S., Doniach, S., Uversky, V. N., and Fink, A. L. (2003) Partially folded intermediates in insulin fibrillation, *Biochemistry 42*, 11404−11416.
41. Goto, Y., and Fink, A. L. (1989) Conformational states in β-lactamase: Molten-globule states at acidic and alkaline pH with high salt, *Biochemistry 28*, 945−952.
42. Semisotnov, G. V., Rodionova, N. A., Razgulyaev, O. I., Uversky, V. N., Gripas, A. F., and Gilmanshin, R. I. (1991) Study of the "molten globule" intermediate state in protein folding by a hydrophobic fluorescent probe, *Biopolymers 31*, 119−128.
43. Ptitsyn, O. B. (1995) Molten globule and protein folding, *Adv. Protein Chem. 47*, 83−229.
44. Arai, M., and Kuwajima, K. (2000) Role of the molten globule state in protein folding, *Adv. Protein Chem. 53*, 209−282.
45. Poklar, N., Lah, J., Salobir, M., Macek, P., and Vesnaver, G. (1997**)** pH and Temperature-Induced Molten Globule-Like Denatured States of Equinatoxin II: A Study by UV-Melting, DSC, Far- and Near-UV CD Spectroscopy, and ANS Fluorescence, *Biochemistry 36*, 14345−14352.
46. Bryant, C., Strohl, M., Green, L. M., Long, H. B., Alter, L. A., Pekar, A. H., Chance, R. E., and Brems, D. N. (1992) Detection of an equilibrium intermediate in the folding of a monomeric insulin analog, *Biochemistry 31*, 5692−5698.
47. Millican, R. L., and Brems, D. N. (1994) Equilibrium intermediates in the denaturation of human insulin and two monomeric insulin analogs, *Biochemistry 33*, 1116−1124.

48. Bouchard, M., Zurdo, J., Nettleton, E. J., Dobson, C. M., and Robinson, C. V. (2000) Formation of insulin amyloid fibrils followed by FTIR simultaneously with CD and electron microscopy, *Protein Sci. 9*, 1960−1967.
49. Walsh, D. M., Lomakin, A., Benedek, G. B., Condron, M. M., and Teplow, D. B. (1997) Amyloid β-Protein Fibrillogenesis. Detection of a protofibrillar intermediate, *J. Biol. Chem. 272*, 22364−22372.
50. Harper, J. D., and Lansbury, P. T., Jr. (1997) Models of amyloid seeding in Alzheimer's disease and scrapie: Mechanistic truths and physiological consequences of the time-dependent solubility of amyloid proteins, *Annu. Rev. Biochem. 77*, 385−407.
51. Walsh, D. M., Klyubin, I., Fadeeva, J. V., Cullen, W. K., Anwyl, R., Wolfe, M. S., Rowan, M. J., and Selkoe, D. J. (2002) Naturally secreted oligomers of amyloid β protein potently inhibit hippocampal long-term potentiation in vivo, *Nature 416*, 535−539.
52. Hong, D. P., Gozu, M., Hasegawa, K., Naiki, H., and Goto, Y. (2002) Conformation of β_2-Microglobulin Amyloid Fibrils Analyzed by Reduction of the Disulfide Bond, *J. Biol. Chem. 277*, 21554−21560.

BI0604936